ChemComm

Accepted Manuscript

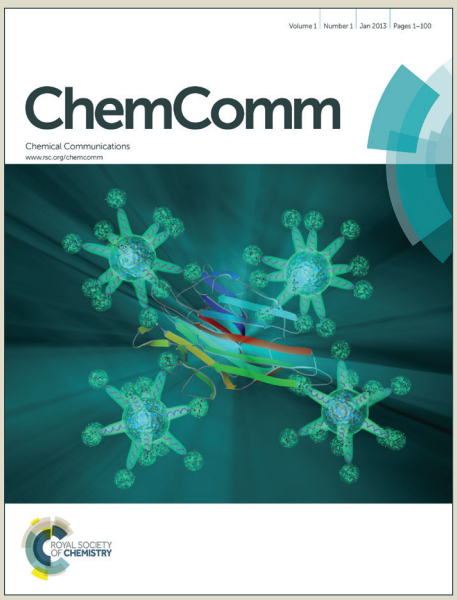

ROYAL SOCIETY OF CHEMISTRY

www.rsc.org/chemcomm

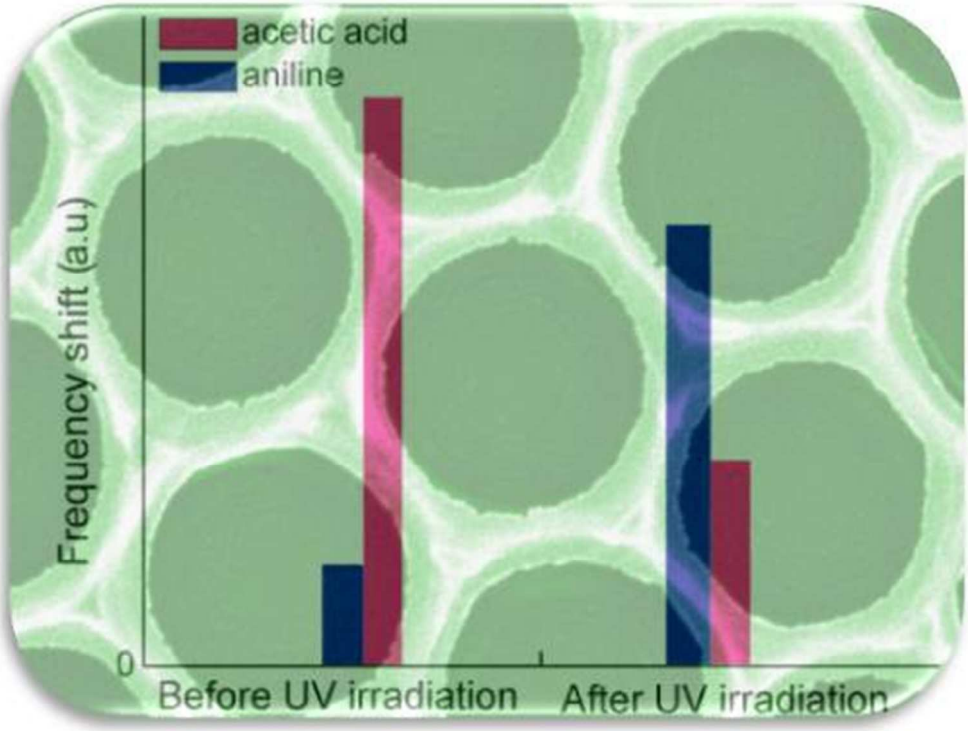

111x80mm (117 x 124 DPI)

Submitted to Chem Commun

The table of contents entry

Keyword (macro-mesoporous, Sensing, film)

Lichao Jia, Hongqiang Wang, Dattatray Dhawale, Chokkalingam Anand, Mohammad A. Wahab, Qingmin Ji, Katsuhiko Ariga and Ajayan Vinu

Highly Ordered Macro-mesoporous Carbon Nitride Film for Selective Detection of Acidic/Basic Molecules

Here we report on the preparation and its "photo-switch" sensing performance of meso-macroporous carbon nitride film for both acidic and basic molecules.

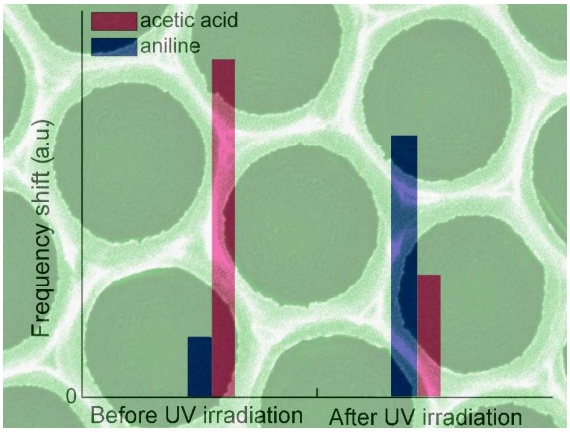

Chemical Communications RSCPublishing

COMMUNICATION

Highly Ordered Macro-mesoporous Carbon Nitride Film for Selective Detection of Acidic/Basic Molecules

Cite this: DOI: 10.1039/x0xx00000x

Lichao Jia,[a,] Hongqiang Wang,[b] Dattatray Dhawale,[a,c] Chokkalingam Anand,[a,c] Mohammad A. Wahab,[c] Qingmin Ji,[c] Katsuhiko Ariga[a,b] and Ajayan Vinu[c]

Received 00th January 2014,
Accepted 00th January 2014

DOI: 10.1039/x0xx00000x

www.rsc.org/

Well-ordered meso-macroporous carbon nitride film fabricated via a simple and flexible template replication method by using P_{123} block copolymer and polystyrene spheres as dual templates shows a selective sensing performance for acetic acid but after treating the surface of the film with UV light and oxygen, the selectivity of sensing can be tuned for basic molecule.

Carbon nitride (CN) materials have attracted great technological interest during the last few decades because of their excellent physico-chemical properties including high toughness, low friction coefficient, reliable chemical inertness, semi-conductivity, intercalation ability, high thermal conductivity, and oxygen and/or water resistivity.[1,2] Owning to the unique properties, these superhard materials, predicted to be as hard as diamond, promise a variety of technological and biological applications, such as biocompatible coatings on biomedical implants, battery electrodes, gas-separation systems, corrosion protection, catalysis, molecule adsorption, and gas sensors.[3-9]Since these applications directly depend on the structure and texture parameters including surface area, pore volume, and well-ordered porous structure that can offer a lot of active or adsorption sites, considerable effort has been dedicated to introduce micro or mesoporosity in the CN wall structure.[10-13] This was first realized by Vinu and his co-workers who reported the carbon nitride with a well-ordered mesoporous structure and excellent textural parameters through a simple polymerization reaction between ethylenediamine and carbon tetrachloride by a nanocasting technique using SBA-15 as a hard template.[14] The same group also reported the different ways to control of the pore diameter, crystallinity, band gap, and the nitrogen content of the CN materials and demonstrated extensively their performance in various base catalyzed transformation.[14] Since these materials offer potential application possibilities in various fields, many researchers have turned their attention to this area and reported different ways of preparing the porous carbon nitride samples and investigated their performance in catalysis, energy storage, and hydrogen evolution. Especially, Antonietti et al. made a significant contribution to this research and demonstrated the synthesis of porous carbon nitride nanoparticles, and polymeric CN networks, and their application in catalysis and photocatalysis.[3,10,15] However, most of the works are related with the porous carbon nitride in powder form that restricts their application possibilities, As the carbon nitride films are of importance for semiconducting devices, sensors, fuel cells, and energy storage applications, synthesis of CN films has been receiving a lot of attention, and can be fabricated by several techniques including radio frequency plasma deposition, pulsed laser ablation in a vacuum, ion-beam-assisted deposition, ion implantation, and magnetron sputtering.[16] Although these techniques offer non-porous CN films with controllable film thickness, composition and particle size by simply tuning the experimental parameters, the non-porosity, poor textural features including a low specific surface area, and less ordered porous structure may greatly limit their potential in electronic and sensing applications. Even though this can be overcome by introducing nanoporosity in the CN film structure, to the best of our knowledge, no studies have been reported so far on the fabrication of macro-mesoporous carbon nitride films with a bimodal pore system. It is not easy to create nanoporosity in the film with CN framework as it requires a unique strategy to create the films without any defect sites and a high nitrogen content.

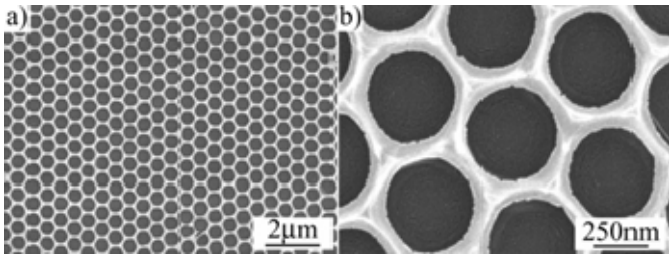

Fig. 1. FESEM Images of macro-mesoporous CN film from top view: (a) low-magnification, (b) high-magnification.

Herein, we report a simple and flexible approach for the fabrication of well-ordered macro-mesoporous CN film by using the combination of soft- and hard-templating approach in which polystyrene spheres (PS) and P123 block copolymer were used as structuring agents and a polymeric precursor, polyethylenimine (Figure S1). Macropores are generated by PS spheres whereas the mesoporosity is obtained from the self-assembled P123 and silica nanocomposite filled with polyethylenimine (soft-templating) that is bonded with the PS spheres via hard-templating approach. This dual strategy offered both macro and mesoporosity in the CN network. In addition, the prepared highly ordered novel macro-mesoporous CN film is dark brown in color and showed excellent adsorption capability for acidic molecules. Interestingly, the adsorption properties can be tuned with a simple treatment of UV light and oxygen that generates COOH and N-oxide groups on the surface. The surface COOH and N-oxide groups could finally help to tune the selectivity of the adsorption to basic molecules.

Typical scanning electron microscopy (SEM) images after annealing at 450 °C shown in Figure 1 highlight the formation of a continuous macro-mesoporous CN film extending over several μm in length and a long-range structural ordering of the macroporous CN framework derived from the ordered lattice of polystyrene spheres. The SEM images also reveal that the macropores are separated by thick CN walls that are perfectly arranged without many cracks on the surface. It should be noted that the diameter of the macropore is about 470 nm, which is similar with that of 476 nm PS beads used in the synthesis. The small shrinkage is attributed to the removal of PS spheres and the condensation or shrinkage of silica and the CN framework walls. The average thickness of the walls between adjacent pores was about 80 nm. Interestingly, ordered mesopores can be clearly seen in the high magnification SEM image (Figure 1b) with concentric structural circles, indicating that this material has ordered mesoporous structure within the curved shells. Further, the mesostructure can be confirmed and seen more clearly from transmission electron microscopy (TEM) image (Figure S2a) and small angle XRD shown in Figure S3. From the enlarged image of the single pore wall (curved shell, shown in Figure S2b), the macroporous CN framework clearly comprises of well-defined mesochannels that are originated from the self-assembled P123 surfactant and silica nanostructures. The formation of macro-mesostructure indicates that the CN precursor can easily cover on the macropore template of PS spheres and immerse in the mesopore template of P123 surfactant and silica nanostructures. Upon the calcination and HF treatment, the PS spheres, P123 surfactant and the mesoporous silica framework can be removed. The presence of both the meso and macropores in the CN framework, not only increases the surface area, but also aids the penetration of reactive species. A broad peak at 25.8° in the XRD pattern (Figure S3) with the corresponding interlayer d spacing of 0.342 nm, which is often related to the turbostratic ordering of carbon and nitride atoms in the graphene layers, indexed as the (002) plane for graphitic material, confirms the graphitic CNs phase in the macro-mesoporous CN film.[4b, 14]

To further confirm the presence of CN network on the wall structure of the film, the elemental mapping of the mesoporous CN film was done and the images are shown in Figure 2. Obviously, the morphology of carbon and nitrogen is similar with the SEM and TEM images shown in Figure 1 and S2, indicating the presence of CN network in the walls surrounded by the macropores and the homogeneous distribution of these C and N on both the exterior and interior surfaces of the sample. This is mainly attributed to the perfect filling of the CN precursors into the P123/silica and PS nanostructure. The corresponding electron energy loss spectrum (EELS) of the specimen is illustrated in Figure 2d, which obviously reveals the presence of ionization edges located at 284 and 401 eV, indexed as C and N K edges, respectively. The strong signals of C and N and the absence of the peaks related with Si and O indicate that the sample is composed of only CN network and the macro and mesoporosity are generated from the PS spheres and silica. The peak at 284 eV is due to 1s- π^* electron transitions and attributed to sp^2-hybridized carbon bonded to nitrogen, which is mainly caused by the higher electronegativity of nitrogen that decreases the electron density on the C atoms.[17] For the N K-edge, the peak state is similar to that of the C K-edge of the sample, which attributes the S-triazine based graphitic carbon nitride network.[11a] The carbon to nitrogen ratio obtained from the EEL spectrum was calculated to be 3.5, which is lower than the carbon to nitrogen ratio of the MCN-1 powder sample that was prepared by using ethylenediamine and carbon tetrachloride.[14]

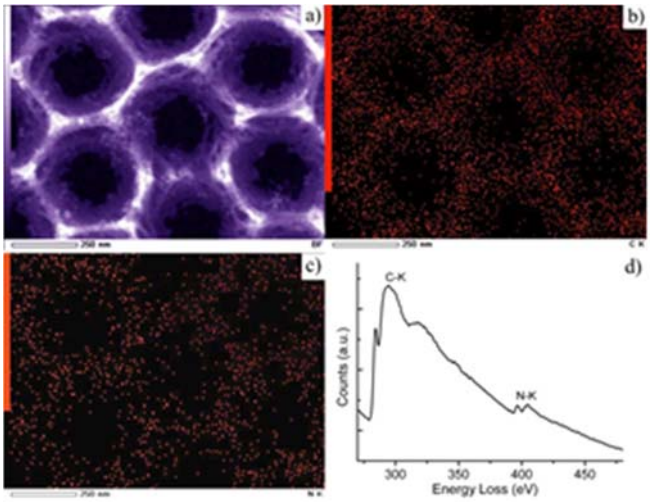

Fig. 2. (a-c) EELS mapping images of macro-mesoporous CN film: (a) bright-filed image, (b) carbon, (c) nitrogen. (d) EELS spectra.

As given in Figure 3, X-ray photoelectron spectroscopy (XPS) of the CN was used to obtain further information about the chemical bonds. The C1s spectrum in the Figure 3a reveals the presence of three kinds of carbon atom in our sample, whose components have peaks at about 284.17, 285.4 and 288.06 eV. The lowest energy contribution located at 284.17 eV is assigned to pure graphitic sites in the amorphous CN matrix and C-H bond that normally comes from the contamination[14b] whereas the peak centered at 285.4 eV is attributed to the sp^2 C atoms bonded to N inside the aromatic structure.[11b] The highest energy contribution around 288.06 eV corresponds to the sp^2-hybridized carbon in the aromatic ring attached to the NH or NH_2 group.[16b] For the N 1s spectrum, it can be fitted as two peaks at binding energies of 397.9 and 400.01 eV, indicating the presence of at least two different chemical environments for N atoms that are attached with C. It is assumed that one N is linked with aromatic structure whereas other nitrogen is connected with the different aromatic micro domains or terminal nitrogen attached with the outside of the aromatic ring. The peak centered at 397.9 eV corresponds to electrons originating from nitrogen atoms sp^2-bonded to carbon or, more precisely, to nitrogen atoms in C=N-C groups.[18a] The predominant component with binding energy of 400.01 eV can be attributed to N atoms trigonally boned to all sp^2 carbons, or to two sp^2 carbon atoms and N-terminal groups in an amorphous C-N network.[18b] These results are in good agreement with the results obtained for the C1s spectra. In addition, the amount of nitrogen calculated from the XPS analysis is also consistent with the value obtained from the EELS analysis, confirming that the nitrogen is bonded with carbon and uniformly distributed. However, the ratio of carbon to nitrogen of our sample can significantly be changed when varying the carbonization temperature as demonstrated

in Figure S4. This ratio gradually increases from 3.5 to 8.2 with the increasing carbonization temperature from 450 to 600 °C. The huge reduction in the nitrogen content with increasing carbonization temperature could be mainly due to the fact that the nitrogen atoms from the polymerized matrix are released as the thermodynamic stability of N in the carbon matrix is very low and it prefers to stay as molecule at a high temperature. The surface chemical-bonding state of the materials was characterized by FT-IR spectroscopy (see in Figure S5). The overall features of the spectrum are similar to those of other CN systems with the absorption between 500 cm^{-1} and 950 cm^{-1} that can be assigned to the out-of-plane bending mode for graphite-like sp^2 domains, and the peaks at 1436 cm^{-1} and 1620 cm^{-1} that can be assigned to aromatic C-N stretching mode and C=N stretching, respectively.[19]

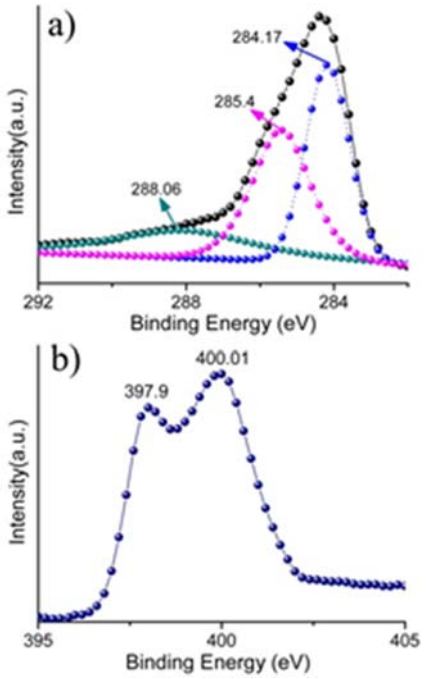

Fig. 3. (a) C1s and (b) N1s XPS spectra of macro-mesoporous CN.

It is well known that establishing detection techniques of environmentally hazardous substances is one of the most crucial issues currently and mesoporous CN material is the most promising candidate for this kind of application.[20] Thus, the adsorption performance of various volatile substances for our sample was investigated by quartz crystal microbalance (QCM) resonator. As illustrated in Figure 4, several adsorbents including acetic acid, aniline, propanol, acetone, ethyl acetate, cyclohexane and toluene were chosen as guest substances. In QCM, the decrease of QCM frequency is proportional to the increase of mass for the tested volatile substances. Among the adsorbates used, acetic acid shows the greatest affinities towards CN films and the adsorbed amount at equilibrium is almost 6 times larger than that of aniline, indicating the high selectivity to molecule with acid functionality, which is mainly attributed to the presence of basic nitrogen groups onto the carbon framework such as NH, NH_2, or N bonded with the carbon matrix in the wall structure of the CN film.[5b] Surprisingly, after irradiating the sample with UV light in oxygen atmosphere that generates ozone, the selectivity of CN material between acid and base is completely reversed as shown in Figure 4b. After the ozone treatment, the sample displays a high affinity to aniline but not to acetic acid, indicating that the selectivity for these two guests can be easily controlled by functionalizing the surface of materials. In other words, the selectivity of the film can easily be tuned by UV light irradiation and the sample behaves as "Photo Switch Sensor": high sensitivity towards acetic acid without UV irradiation while a surprising selectivity to aniline after flashing with UV light in oxygen, as UV irradiation in oxygen generates COOH groups on the CN film surface.[20c]This is confirmed by the fact that the FT-IR spectrum of the oxidised sample displays a broad peak at 3100-3600 cm^{-1} which is attributed to the OH stretching of carboxyl groups that are originated from the oxidation of amorphous carbon in the CN wall structure. It is also interesting to note that the oxidized sample shows a sharp peak at 1230 cm^{-1} which is assumed to come from the oxidation of primary amines or tertiary amine groups on the surface the CN walls into N-oxide groups which may also strongly interact with amines (Figure S6). The broad IR absorption around 2000cm^{-1} could be assigned to hydroxylamines (-NHOH) and cyanates (C=N=O). From these data, it can be concluded that the oxidation of the CN nanostructure by ozone creates functional moieties on the surface that help the selective adsorption of amine molecules. Because of these exciting properties together with a high surface area, a large pore diameter, and large pore volume, it is expected that these materials can also offer excellent results in other volatile substances.

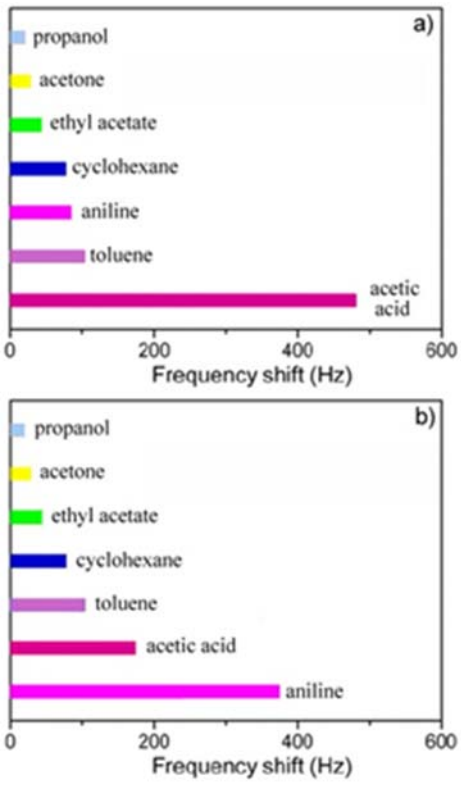

Fig. 4. QCM frequency shift of macro-mesoporous CN film upon absorption of various volatile substances. (a) before and (b) after UV light irradiation in oxygen.

Actually, the present efficient strategy reported in this communication is universal and flexible. For example, the texture and structure parameters can be easily manipulated by choosing the polystyrene spheres with different diameters to control the macropore size, or changing the drying temperature of P123 block copolymer to tune the mesopore size, or varying the layer number of colloidal template to control the thickness of the film.[14,21-22] Representatively, monolayered CN films with 200 nm and 1000 nm macropore size are shown in Figure S6a and 6b, respectively. The microstructures of all CN films are similar except the pore size. It is also envisaged that CN films with

different dopants (such as Ti-CN, Fe-CN, Pt-CN etc.) can be fabricated by adding doped ions into the precursor solution. The corresponding performance of the CN material can be utilized in many fields, such as catalysis, adsorption, battery electrodes, gas sensing and so on.[21] In addition, based on the transferability of colloidal template in the water, all of these films can be directly constructed on any desired substrate with flat or curved surfaces, which can greatly enlarge the application fields of porous CN film and provide the possibility for the creation of CN device.[22]

In conclusion, macro-mesostructurally patterned and well-ordered CN film with uniform mesoporous wall has been fabricated using a simple and flexible template replication method by combination of P123 block copolymer and monodispersed polystyrene spheres as dual templates. The prepared films have both macro and mesoporous that are arranged in an orderly fashion throughout the sample. The macropore size and the thickness of the film can be controlled with a simple adjustment of the size of PS spheres whereas the nitrogen content can be tuned with tuning the carbonization temperature. Interestingly, the obtained sample offers superior affinity for acetic acid, however, after flashing with UV light and oxygen, the adsorption selectivity towards aniline and acetic acid is reversed. We envisage that these interesting features of the film make a significant breakthrough in the field of sensors and could lead to make novel organic electronics or sensors.

Notes and references

[a]Australian Institute for Bioengineering and Nanotechnology, The University of Queensland, 75, Corner College and Cooper Rds, St Lucia, QLD 4072, Australia, E-mail: a.vinu@uq.edu.au.

[b]International Center for Materials Nanoarchitectonics

National Institute for Materials Science, 1-1 Namiki, Tsukuba 305-0044, Ibaraki, Japan.

[c]Nanosystem Research Institute (NRI), National Institute of Advanced Industrial Science and Technology (AIST)

1-1-1 Higashi, Tsukuba 305-8565, Ibaraki,Japan.

Electronic Supplementary Information (ESI) available: [Experimental section, and the detailed characterization data of the prepared materials including FT-IR, nitrogen content, XRD pattern and TEM images are included. See DOI: 10.1039/c000000x/

Acknowledgement:

One of the authors, Chokkalingam Anand acknowledges the CMM (Centre for Microscopy and Microanalysis – AMMRF) for providing the state of art microscope facilities. One of the authors, Ajayan Vinu is grateful to ARC for the award of the future fellowship and the University of Queensland for the start-up grant.

1 (a) A. Y. Liu and M. L. Cohen, *Science,*1989,**245,** 841-842;(b) A. Y. Liu and R. M. Wentzcovitch, *Phys. Rev. B,*1994,**50,** 10362-10365; (c) D. M. Teter and R. J. Hemley, *Science,*1996,**271,** 53-55; (d) C. M. Sung and M. Sung, *Mater. Chem. Phys.*,1996, **43,** 1-18; (e) J. V. Badding, *Adv. Mater.*,1997,**9,** 877-886; (f) R. C. DeVries, *Mater. Res. Innovat.*,1997, **1,** 161-162.

2 a) V. N. Khabashesku, J. L. Zimmerman and J. L. Margrave, *Chem. Mater.*,2000, **12,** 3264-3270; (b) M. H. V. Huynh, M. A. Hiskey, J. G. Archuleta and E. L. Roemer, *Angew. Chem. Int. Ed.*,2005,**44,** 737-739; (c) D. J. Li and L. F. Niu, *Bull. Mater. Sci.*,2003, **26,** 371-375.

3 (a) X. C. Wang, K. Maeda, A. Thomas, K. Takanabe, G. Xin, J. M. Carlsson, K. Domen and M. Antonietti, *Nat. Mater.*,2009,**8,** 76-82; (b) Y. J. Zhang, A. Thomas, M. Antonietti and X. C. Wang, *J. Am. Chem. Soc.*,2009, **131,** 50-52.

4 (a) K. K. R. Datta, B. V. S. Reddy, K. Ariga and A.Vinu, *Angew. Chem. Int. Ed.*,2010,**49,** 5961-5965; (b) X. Jin, V. V. Balasubramanian, S. T. Selvan, D. P. Sawant, M. A. Chari, G. Q. Lu and A. Vinu, *Angew. Chem. Int. Ed.*,2009, **48,** 7884-7887.

5 (a) L. M. Zambov, C. Popov, N. Abedinov, M. F. Plass, W. Kulisch, T. Gotszalk, P. Grabiec, I. W. Rangelow and R. Kassing, *Adv. Mater.*,2000,**12,** 656-660; (b) G. P. Hao, W. C. Li, D. Qian and A. H. Lu, *Adv. Mater.*,2010,**22,** 853-857.

6 (a) P. Y. T essier, L. Pichon, P. Villechaise, P. Linez, B. Angleraud, N. Mubumbila, V. Fouquet, A. Straboni, X. Milhet and H. F. Hildebrand, *Diam. Relat. Mater.*,2003,**12,** 1066-1069; (b) E. Broitman, W. Macdonald, N. Hellgren, G. Radnóczi, Zs. Czigány, A. Wennerberg, M. Jacobsson and L. Hultman, *Diam. Relat. Mater.*,2000,**9,** 1984-1991.

7 C. Donnet and A. Erdemir, *Surf. Coat. Technol*.,2004,**180/181,** 76-84.

8 M. Kim, S. Hwang and J. S. Yu, *J. Mater. Chem*.,2007,**17,** 1656-1659.

9 E. Broitman, G. K. Gueorguiev, A. Furlan, N. T. Son, A. J. Gellman, S. Stafström and L. Hultman, *Thin Solid Films*,2008,**517,** 1106-1110.

10 (a)Y. S. Jun, W. H. Hong, M. Antonietti and A. Thomas, *Adv. Mater*.,2009,**21,** 4270-4274; (b) X. Chen, Y. Jun, K. Takanabe, K. Maeda, K. Domen, A. Thomas, X. Fu, M. Antonietti and X. Wang, *Chem. Mater*.,2009,**21,** 4093-4095.

11 (a)Y. C. Zhao, Z. Liu, W. G. Chu, L. Song, Z. X. Zhang, D. L. Yu, Y. J. Tian, S. S. Xie and L. F. Sun, *Adv. Mater*.,2008, **20,** 1777-1781; (b) Y. G. Li, J. Zhang, Q. S. Wang, Y. X. Jin, D. H. Huang, Q. L. Cui and G. T. Zou, *J. Phys. Chem. B*,2010,**114,** 9429-9434; (c) H. Q. Wang, G. Z. Wang, L. C. Jia, C. J. Tang and G. H. Li, *J. Phys. D Appl. Phys*.,2007, **40,** 6549-6553.

12 S. W. Bian, Z. Ma and W. G. Song, *J. Phys. Chem. C*,2009,**113,** 8668-8672.

13 (a) J. L. Zimmerman, R. Williams, V. N. Khabashesku and J. L. Margrave, *Nano Lett*.,2001, **1,** 731-734; (b) H. Q. Wang, G. H. Li, L. C. Jia, G. Z. Wang and C. J. Tang, *J. Phys. Chem. C*,2008,**112,** 11738-11743.

14 (a) A. Vinu, K. Ariga, T. Mori, T. Nakanishi, S. Hishita, D. Golberg and Y. Bando, *Adv. Mater*.,2005,**17,** 1648-1652; (b) A. Vinu, *Adv. Funct. Mater*.,2008,**18,** 816-827.

15 Y. Wang, J. S. Zhang, X. C. Wang, M. Antonietti and H. R. Li, *Angew. Chem. Int. Ed*.,2010,**49,** 3356-3359.

16 (a) J. J. Wang, D. R. Miller and E. G. Gillan, *Chem. Commun*.,2002, 2258-2259;(b) A. Majumdar, G. Scholz and R. Hippler, *Surf. Coat. Technol*.,2009, **203,** 2013-2016.

17 A. Vinu, S. Anandan, C. Anand, P. Srinivasu, K. Ariga and T. Mori, *Microporous Mesoporous Mater.*,2008, **109,** 398-404.

18 a) A. Thomas, A. Fischer, F. Goettmann, M. Antonietti, J. Müller, R. Schlögl and J. M. Carlsson, *J. Mater. Chem.*,2008,**18,** 4893-4908; (b) Y. H. Cheng, B. K. Tay, S. P. Lau, X. Shi, X. L. Qiao, J. G. Chen, Y. P. Wu, Z. H. Sun and C. S. Xie, *J. Mater. Res*., 2002,**17,** 521-524.

19 L. Liu, D. Ma, H. Zheng, X. J. Li, M. J. Cheng and X. H. Bao, *Microporous Mesoporous Mater*.,2008,**110,** 216-222.

20 (a) K. Ariga, A. Vinu, Q. M. Ji, O. Ohmori, J. P. Hill, S. Acharya, J. Koike and S. Shiratori, *Angew. Chem. Int. Ed*.,2008,**47,** 7254-7257; (b) Q. M. Ji, S. B. Yoon, J. P. Hill, A. Vinu, J. S. Yu and K. Ariga, *J. Am. Chem. Soc*.,2009, **131,** 4220-4221; (c) L. C. Jia,G. P. Mane, C. Anand, D. S. Dhawale, Q. M. Ji, K. Ariga and A.Vinu, *Chem. Commun*.,2012, **48,** 9029-9031.

21 L. C. Jia, W. P. Cai and H. Q. Wang, *Appl.Phys.Lett.*,2010, **96,** 1031151-3.

22 (a) L. C. Jia, W. P. Cai and H. Q. Wang, *J. Mater. Chem*.,2009,**19,** 7301-7307; (b) L. C. Jia, W. P. Cai, H. Q. Wang, F. Q. Sun and Y. Li, *ACS Nano*,2009, **3,** 2697-2705.

